Int. J. Multiphase Flow Vol. 12, No. 3, pp. 459–468, 1986
Printed in Great Britain

0301-9322/86 $3.00 + .00
Pergamon Journals/Elsevier

ROTATIONAL AND TRANSLATIONAL MOTION OF A SPHERE PARALLEL TO A WALL

K. MAŁYSA† and T. G. M. VAN DE VEN
Pulp and Paper Research Institute of Canada and Department of Chemistry, McGill University, 3420 University St, Montreal, Quebec H3A 2A7, Canada

(*Received* 29 *April* 1985; *in revised form* 15 *August* 1985)

Abstract—Rotational and translational velocities of a sphere moving parallel to a plane wall were determined experimentally as a function of wall–sphere separation. The measurements were carried out under creeping flow conditions for dimensionless gap widths ϵ in the range 0.006–1.8. Good agreement between the experimental data and the results calculated from exact solutions was found for the whole range of gap widths investigated. The ranges of applicability of solutions by the method of reflections and by lubrication theory are discussed.

INTRODUCTION

In most environmental and industrial flows, particles suspended in the fluid phase are commonly encountered. Normally the flow takes place in a confined space (pipes, channels, etc.) The presence of walls has a significant effect on the motion of particles close to the wall. Wall–particle hydrodynamic interactions are a reflection of changes, caused by the presence of a wall, in the long-range velocity field in the fluid surrounding each moving particle. Due to the presence of a wall, the velocity distribution around a moving particle becomes asymmetric, thus changing the particle mobility. Near a solid wall the particle mobility decreases, and as a result of the asymmetric flow field, particles moving parallel to a wall rotate. Changes in particle mobility near an interface can significantly influence the kinetics of various processes such as, for example, particle deposition on collectors or other surfaces, surface coagulation, particle diffusion through an interface, etc., in which there is a stage when particles approach an interface.

The effect of a wall on the motion of particles under creeping flow conditions has been discussed by Happel & Brenner (1965). Recently, Hirschfeld *et al.* (1984) reviewed the literature of the subject with emphasis on the motion of arbitrarily shaped particles within a circular cylinder. Despite a significant number of theoretical papers dealing with wall effects, exact solutions valid for all particle–wall separations are available only for a single spherical particle approaching or moving parallel to an interface. Dean & O'Neill (1963) succeeded in solving the Stokes equations for the rotation of a sphere about an axis parallel to a nearby plane wall bounding a semi-infinite fluid. O'Neill (1964) gave the solution for translation of the sphere parallel to the wall. Goldman *et al.* (1967) found that the numerical data computed by Dean & O'Neill (1963) contained errors. They obtained results for small gap widths using lubrication theory, and they also corrected Dean & O'Neill's computations. Goldman *et al.* (1967) compared their theoretical predictions with the experimental data available at that time given by Carty (1957). They found no agreement and concluded that cavitation of the fluid in Carty's measurements of the terminal velocities of spherical particles rolling down a smooth plate was the most likely reason for the disagreement. Recently, Ambari *et al.* (1983) measured the translational velocity of a sphere moving parallel to a wall, and they reported a lack of agreement of the experimental results with O'Neill's (1964) exact solution. Their experimental data were in fair agreement, especially for small wall–sphere gap widths, with Faxen's (1921) solution obtained by the method of reflections. These findings are rather surprising because the method of reflections is only valid for large gap widths. As far as we are aware, no experimental data for the rotation of a sphere moving parallel to a wall has been reported in the literature.

† On leave from the Institute of Catalysis & Surface Chemistry, Polish Academy of Sciences, Krakow, Poland.

This paper presents results of measurements of the rotational and translational velocities of a sphere moving parallel to a solid wall. Experimental results are compared with predictions of various theoretical approaches: exact solutions, lubrication theory and solutions by the method of reflections. Ranges of agreement of the theoretical approaches with the experimental data for the sphere rotation and translation are shown and discussed.

THEORY

Let us consider a solid sphere of radius a (see figure 1) moving (under creeping flow conditions) in the negative z-direction parallel to and at a distance h from a solid plate located in the xz plane. The sphere moves under the action of gravity force F^g in an otherwise quiescent fluid. As a result of the presence of a wall, the sphere translates parallel to the wall with velocity $V_z = -(\mathrm{d}z\ \mathrm{d}t)$ and rotates with angular velocity $\omega = \mathrm{d}\theta'/\mathrm{d}t$ (see figure 1). Both velocities V_z and ω are a function of the wall–sphere gap with $\epsilon = h/a$. The hydrodynamic reactive force F and torque T_x (about the sphere center) exerted by the fluid on the sphere translating and rotating near a wall can be expressed as

$$F_z = -6\pi\mu a\ (V_z f^t + a\omega f^r)\ , \qquad [1]$$

$$T_x = -8\pi\mu a^2\ (V_z t^t + a\omega t^r)\ , \qquad [2]$$

where f^t, f^r, t^t and t^r are resistance coefficient corrections arising from the wall. The resistance coefficient corrections f^t, f^r, t^t and t^r are nondimensional quantities which are only a function of the gap width ϵ. In the case of a neutrally buoyant sphere near the wall the torque $T_x = 0$, from [1] and [2] we have

$$\omega = \frac{F_z t^t}{6\pi\mu a^2\ (t^t f^r - t^r f^t)}\ , \qquad [3]$$

$$V_z = \frac{F_z t^r}{6\pi\mu a\ (t^t f^r - t^r f^t)}\ . \qquad [4]$$

To calculate ω and V_z theoretically, we need the values of the resistance coefficients corrections. The problem of a sphere moving parallel to a plane wall is one of the few cases for which exact solutions exist. The numerical values of f^t, f^r, t^t and t^r, obtained by solving the creeping flow equations for translation of the sphere parallel to a plane wall (O'Neill 1964) and for rotation of the sphere about an axis parallel to the wall (Dean & O'Neill

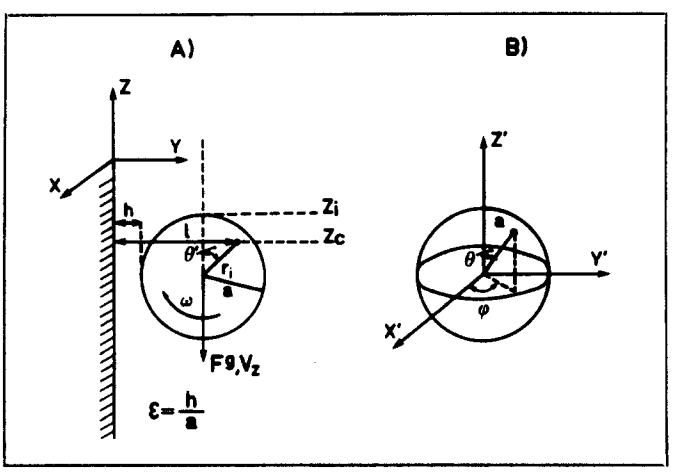

Figure 1. Schematic representation of a sphere sedimenting parallel to a plane wall (A). The rotational velocity ω is determined by the variation in the position of a dot on the surface of the sphere, described by the polar angles θ and ϕ (B). The projection of the dot on the $y'z'$-plane is given by θ' and r_i. ω is determined from variations in θ'.

1963) and recalculated by Goldman *et al.* (1967), were used to calculate the theoretical values of V_x and ω. These theoretically calculated velocities are compared to those determined experimentally.

For more complicated particles and wall geometries no exact solutions exist. Two approaches are commonly applied: (i) solutions using the method of reflections valid for large ϵ, and (ii) the lubrication theory approach valid for $\epsilon << 1$. For a sphere moving parallel to a plane wall, the following relations were obtained from the method of reflections for the resistance coefficient corrections (Goldman *et al.* 1967):

$$f^t = -\left[1 - \frac{9}{16}\left(\frac{1}{\epsilon}\right) + \frac{1}{8}\left(\frac{1}{\epsilon}\right)^3 - \frac{45}{256}\left(\frac{1}{\epsilon}\right)^4 - \frac{1}{16}\left(\frac{1}{\epsilon}\right)^5\right]^{-1}, \quad [5a]$$

$$t^t = \frac{3}{32}\left(\frac{1}{\epsilon}\right)^4\left(1 - \frac{1}{8\epsilon}\right), \quad [5b]$$

$$f^r = \frac{1}{8}\left(\frac{1}{\epsilon}\right)^4\left(1 - \frac{3}{8\epsilon}\right), \quad [5c]$$

$$t^r = -\left[1 + \frac{5}{16}\left(\frac{1}{\epsilon}\right)^3\right]. \quad [5d]$$

From the lubrication theory (Goldman *et al.* 1967), the resistance coefficients corrections are

$$f^t = \frac{8}{15}\ln\epsilon - 0.9588, \quad [6a]$$

$$t^t = -\frac{1}{10}\ln\epsilon - 0.1895, \quad [6b]$$

$$f^r = -\frac{2}{15}\ln\epsilon - 0.2526, \quad [6c]$$

$$t^r = \frac{2}{5}\ln\epsilon - 0.3817. \quad [6d]$$

Results of solutions by the method of reflections and from the lubrication theory are compared to the exact solutions and tested against the experimental data to show the range of their applicability.

EXPERIMENTAL

The experiments were carried out in a plexiglass reservoir of dimensions 42 × 42 × 45 cm filled with a silicone oil (Dow Corning) of density 974 kg/m^3 and viscosity 0.99 Pa at 23°C. A plexiglass plate of size 30 × 35 cm was mounted vertically in the central plane of the reservoir. The reservoir has two viewing windows (14 × 29 cm) made of high-quality optical glass, allowing observation in two perpendicular directions. Nylon spheres of diameter $d = 0.6377 \pm 0.0009$ cm were used in the experiments. The diameter of the spheres was determined using the shadograph technique, by taking an average value of at least 20 measurements at various sphere positions. The sphericity of the spheres used was better than 0.2%. To determine the angular velocity of rotation a small cross was painted on the sphere surface.

The single-frame multiple-image technique was used to record the subsequent positions of the moving sphere. The experimental set-up was illuminated by a stroboscopic lighting system. A stroboscopic lamp was triggered at definite time intervals by an external timing device. A Linhoff camera was used to take pictures. Figure 2 shows examples of some single-frame multiple-image photographs of the sphere moving parallel to the wall. At every

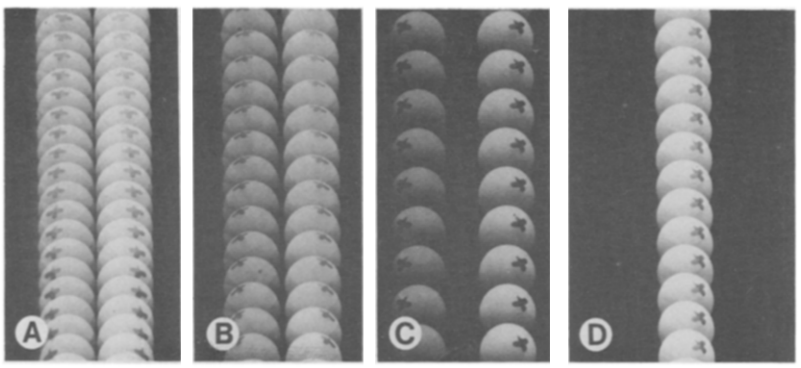

Figure 2. Examples of multiple image single frame photographs of the sphere at various wall–sphere gap widths: (A) $\epsilon = 0.006$, (B) $\epsilon = 0.062$, (C) $\epsilon = 0.544$, (D) $\epsilon \simeq \infty$.

sphere position one can see the mirror image reflected in the vertical plexiglass plate. The diameter of the sphere, the sphere–wall gap and the coordinates of a dot on the sphere surface were measured for every subsequent sphere position. All dimensions and distances were measured with a precision of 0.01 mm using a home-built opticomechanical device. All measured distances and dimensions were normalized with respect to the measured radius a of the sphere image.

At a given sphere position Z_i ($Z_i = z_i/a$), its velocity in the z-direction (cf. figure 1) is given as

$$V_z = \frac{Z_{i+1} - Z_{i-1}}{2\Delta t} \ [\text{radius } s^{-1}] \quad , \qquad [7]$$

where Z_{i+1} and Z_{i-1} are normalized sphere positions neighboring Z_i, and Δt is the time interval between flashes. The angle θ' (figure 1) is, for a given sphere position, determined as

$$\theta' = \sin^{-1}\left[\frac{(l - h - a)}{ar_i}\right] \quad , \qquad [8]$$

where

$$r = \frac{\sqrt{(l - h - a)^2 + (z_c - z_i + a)^2}}{a} \quad , \qquad [9]$$

and h is the gap between the sphere and the wall.

Because the position of the camera is fixed, initially the sphere is observed above the camera axis and subsequently beneath it. Call the angle between the camera optical axis and the line joining the sphere center and the center of the camera objective α (see figure 3). Only when $\alpha = 0$ does the position of the marking dot coincide with that given by [8] and [9]. In general these angles and distances must be corrected for by an amount determined by the angle α.

Consider a dot on a sphere of radius a at orientation (θ,ϕ) with respect to particle fixed coordinates x', y', z' (θ being the angle between the direction of the dot and z', ϕ being the angle between the projection and x', see figure 1). Then the projection of this dot on the space fixed yz-plane is given by

$$\cos\theta' = (1 + \tan^2\theta \sin^2\phi)^{1/2} \quad , \qquad [10]$$

$$r_i = a \cos\theta/\cos\theta' \quad . \qquad [11]$$

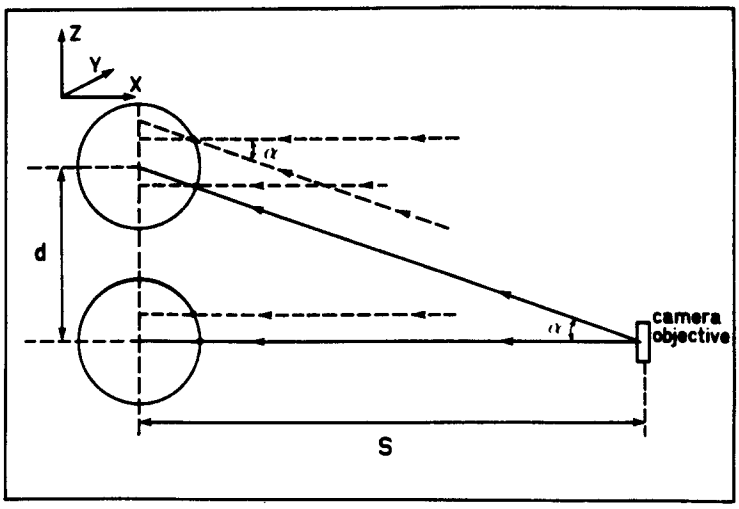

Figure 3. Illustration of deviations in projection of a point at the sphere surface on the plane of observation.

Similarly it can be shown that the projection of the dot on a plane that makes an angle α with the yz-plane is given by

$$\cos\theta'' = f(f^2 + \tan^2\theta \sin^2\phi)^{1/2} \quad , \qquad [12]$$

$$r'' = af \cos\theta/\cos\theta'' \quad , \qquad [13]$$

where

$$f = \cos\alpha + \tan\theta \cos\phi \sin\alpha \quad . \qquad [14]$$

When $\alpha = 0$, [12] and [13] reduce to [10] and [11]. The quantities θ'' and r'' are the ones observed when the sphere is observed under an angle α, while θ' and r_i are the ones that are observed ideally when $\alpha = 0$. From [12] and [13] one can solve for θ and ϕ, and the results can be substituted in [10] and [11]. As the measured angular velocity depends on the angle θ', we are mainly interested in that angle. With the above procedure, one obtains

$$\cos\theta' = \left[1 + \frac{[(r''/a)\sin\theta'']^2}{2A^2 - B \pm 2A(A^2 - B)^{1/2}} \right]^{-1/2} \quad , \qquad [15]$$

where $A = r'' \cos\theta''/a$, and $B = (r''/a)^2(\cos^2\theta'' + \sin^2\theta'' \sin^2\alpha) - \sin^2\alpha$. The $\pm$ sign arises because there are two positions on the sphere which give rise to identical projections.

For small α ($\alpha a << r''$), and defining $\theta'' = \theta' + \Delta\theta$, [15] reduces to

$$\Delta\theta = \alpha\,(a \sin\theta''/r'')\sqrt{1 - (r''/a)^2 \sin^2\theta''} \quad . \qquad [16]$$

Thus a correction $\Delta\theta$ must be applied to the measured angle θ'' given by [15] or [16].

To be precise, a second correction must be applied due to the fact that at finite α the sphere projection deforms in an ellipse. However, this results in a correction of $O(\alpha^2)$ and with our α-values in the range $+5°$ to $-5°$, a deviation from sphericity could not be detected.

The angle α can be determined from

$$\tan\alpha = d/s \quad ,$$

where d is the distance from the sphere center to the optical axis, and s is the distance between the camera and the line of the sedimenting sphere. The distance s can be found

from the relation

$$s = f(1 + m^{-1}) \quad ,$$

where f is the focal length of the camera (13.5 cm) and m the magnification. In our set-up $m = 2.8$.

As a result of observing the sedimentating sphere with a fixed camera, a nonrotating sphere appears to be rotating with an angular velocity $d\Delta\theta/dt$, $\Delta\theta$ given by [16]. This is the case for a sphere far from the wall (in the center of our container). This can be seen from figure 2(D), showing the sedimentation of a sphere far from the wall. Comparing the apparent rotation of a nonrotating sphere with $d\Delta\theta/dt$ yields a good estimate of the experimental error in our experiments. In actual experiments for spheres near a wall the observed angular velocity was corrected for by both the measured apparent velocity far from the wall and [15] or [16]. In all cases the corrected results are very close, and the difference is regarded as a measure of the experimental error.

RESULTS AND DISCUSSION

Changes of the sphere positions as a function of time are shown in figure 4 for various gap widths ϵ. It can be seen that the changes of Z_i vs t are linear. The translational velocity V_z for a given wall–sphere gap width is equal to the slope of the curves, determined by the least square fit. The same method was used to determine the angular velocity ω from the changes of the angle θ' with time t. The $\theta'' = f(t)$ dependence for various gap widths ϵ is shown in figure 5. It can be seen that the scatter in the θ''-values is significantly larger than the observed variations in translational displacement. However, the data in figure 5 are not corrected for the apparent velocity due to the observation by a fixed camera.

The corrected angular velocities are shown in figure 6 together with the estimated experimental error. Changes in the velocity of translation as a function of the gap width ϵ are presented in figure 7, which shows the dependence of the reciprocal mobility U^{-1} vs ϵ. The mobility U is defined as

$$U = V_z/V_\infty \quad , \qquad [17]$$

where V_∞ is the translational velocity of the sphere in an unbounded liquid. In determining the sphere translational velocity the optical deviations discussed above have a negligible

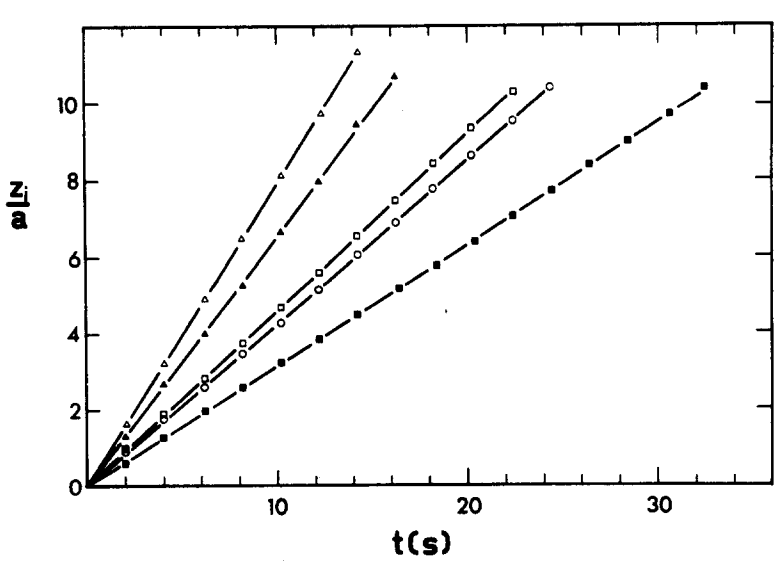

Figure 4. Changes of the sphere position (z_i/a) as a function of time t for various gap widths: (■) $\epsilon = 0.006$; (○) $\epsilon = 0.062$; (□) $\epsilon = 0.102$; (▲) $\epsilon = 0.544$; (△) $\epsilon = 1.45$.

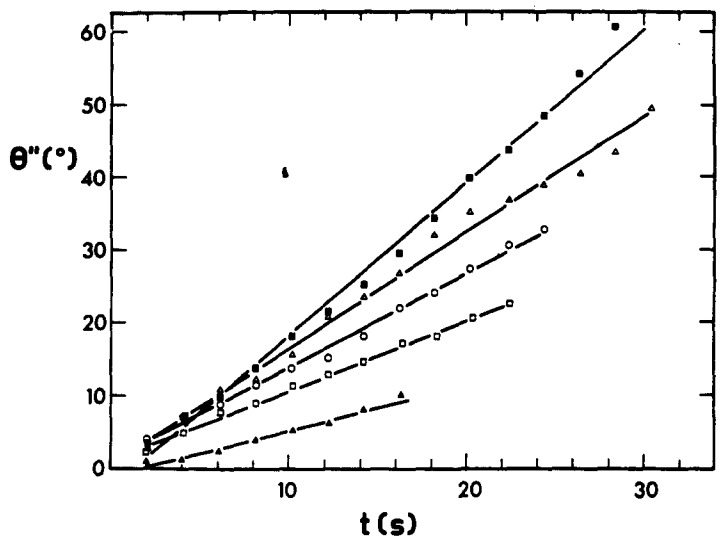

Figure 5. Changes of the apparent angle θ'' as a function of time: (■) $\epsilon = 0.006$; (△) $\epsilon = 0.014$; (○) $\epsilon = 0.062$; (□) $\epsilon = 0.102$; (▲) $\epsilon = 0.544$.

influence on the measured values. At the farthest position from the optical axis (the largest deviation) the deformation of the sphere radius caused by nonperpendicular projections is smaller than 0.4%.

Values of the rotational and translational velocities calculated theoretically are also given in figures 6 and 7, respectively. Curve 1 in figures 6 and 7 represents the exact solutions, curve 2 is calculated from the lubrication theory [3], [4] and [6], and curve 3 is calculated by the method of reflections [3], [4] and [5]. It can be seen that the experimental data are in good agreement with the results predicted by the exact solutions over the whole range of gap widths investigated. Predictions for rotation (figure 6) of the lubrication theory are in good agreement with the experimental data for gap widths $\epsilon < 0.04$. At small gap widths the results calculated by the method of reflections are about two times smaller than the angular velocities determined experimentally. The method of reflections yields angular velocities in agreement with the experimental data for gap widths $\epsilon > 0.3$. Similarly, in the case of the translational velocity V_z (figure 7), the values calculated by the method of reflections (curve 3) are in good agreement with the experimental data for $\epsilon > 0.5$. At gap widths $\epsilon < 0.1$ the lubrication theory (curve 2) describes the experimental data equally as well as the exact solution (curve 1). Thus it can be seen from the data presented in figure 6 and 7 that both limiting approaches, i.e., the lubrication theory and the method of reflections, describe the real situation well in their respective domain of applicability. How-

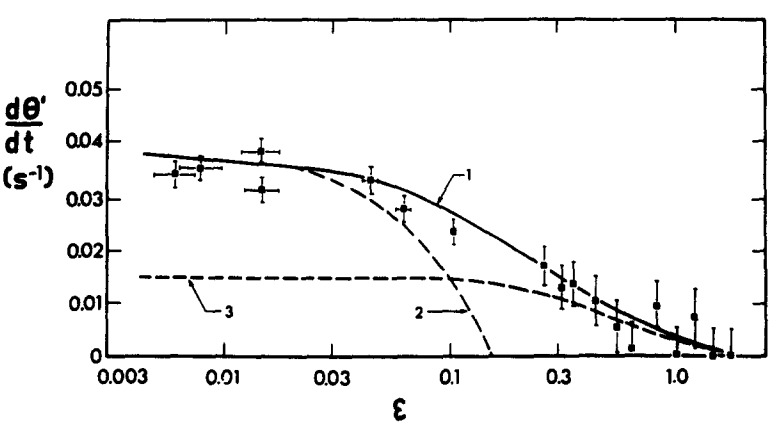

Figure 6. Dependence of the sphere rotation on the gap width. Curve 1, exact solutions; curve 2, lubrication theory; curve 3, method of reflections; (■) experimental data.

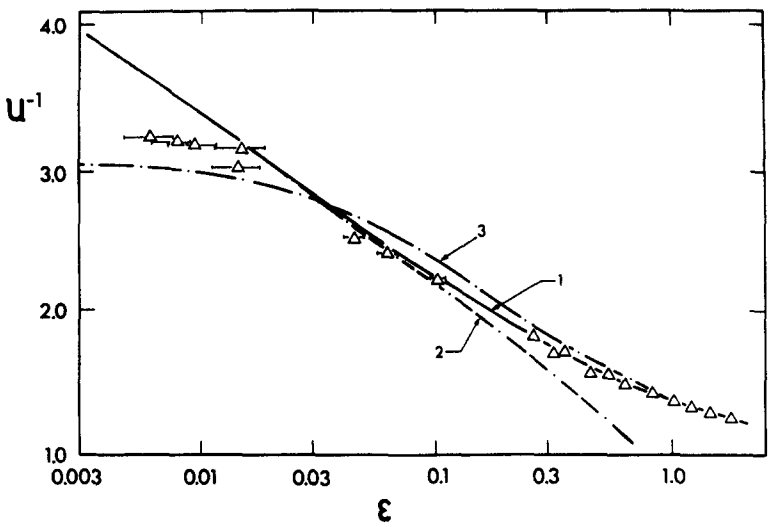

Figure 7. Changes of the reciprocal of sphere mobility U^{-1} with gap width ϵ. Curves 1, 2 and 3 are calculated from the exact solutions, lubrication theory and method of reflections, respectively; (△) experimental data. The vertical error bars are close to the size of the triangles.

ever, there is quite a wide range of the gap widths, $0.03 < \epsilon < 0.3$, where neither of these approaches can properly describe the experimental data.

Our results for translation show deviations from the exact theory, similar to the findings reported recently by Ambari *et al.* (1983). They measured the frictional force exerted on a sphere (diameter $d = 1$ mm) kept by a magnetic field near a wall in the median plane of a cylinder (diameter $D = 10$ mm) moving with constant velocity and reported that at small gap widths, $\epsilon < 0.04$, the experimental data were in agreement with the values calculated by the method of reflections. In their latest paper, Ambari *et al.* (1984) state that the agreement of their data with the results of the method of reflections is probably fortuitous. For the smallest gap investigated, our experimental data for translation (figure 7) also start to deviate from the values predicted by the exact solution and by the lubrication theory towards the values calculated by the method of reflections, but are nevertheless somewhat higher than reported by Ambari *et al.* The difference between observations and theory for small gap widths can be attributed to several factors, the most important ones being: (i) Effects of surface roughness. In our experiments the smallest gap width measured is about 20 μm. The surface roughness of our spheres is of the order of a few micrometers (Małysa *et al.* 1985). In our method we probably measure the outer edge of the roughness profile, so that we underestimate the lowest gap width by a few percent. (ii) Limitations in the sharpness of the outer boundary of the sphere image. This also causes an underestimation of the gap width. (iii) A small deviation from a perfect vertical position of the wall. In case the wall is slightly tilted towards the sedimenting spheres, the sphere will move slightly away from the wall, thus increasing the sedimentation velocity. The combination of these effects can account for the observed differences at small sphere–wall separations. The deviations observed by Ambari *et al.* are probably due to similar causes, and the agreement they claim with the method of reflections is indeed fortuitous. It should be noted that cavitation is absent under our experimental conditions and hence cannot explain the discrepancy. This can be concluded from the estimated pressure in the gap between particle and wall.

Changes of $(-\ \mathrm{d}\theta'/\mathrm{d}z)$ as a function of the gap with ϵ are shown in figure 8. The $(-\ \mathrm{d}\theta'/\mathrm{d}z)$ values represent the ratio of the sphere rotational and translational velocities. It can be seen that within the whole range of gap widths the angular velocity of rotation is much smaller than the velocity of translations. At a gap width of the order of 0.65 the translational velocity is 100 times larger than the velocity of rotation. As a result of an increase in the rotational velocity and a simultaneous decrease in the translational velocity with decreasing gap width ϵ, the $(-\ \mathrm{d}\theta/\mathrm{d}z)$ values approach 0.1 for $\epsilon \simeq 0.02$. The solid

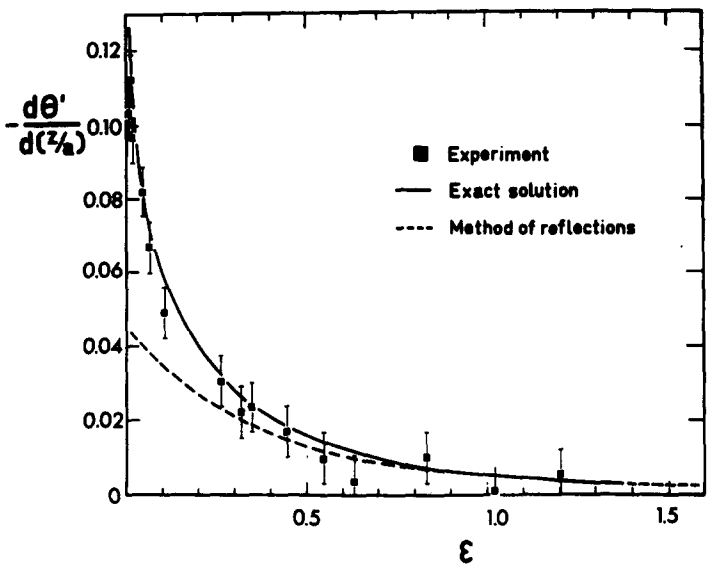

Figure 8. Ratio of the sphere rotational to translational velocities $[-d\theta'/d(z/a)]$ as a function of gap width.

curve in figure 8 represents values obtained from the exact solutions, and the dashed line shows the values calculated by the method of reflections. It can also be seen that the exact solutions describe fairly well the experimental data within the whole range of gap widths. Values calculated by the method of reflections are in agreement with the experimental data only for $\epsilon > 0.3$.

CONCLUDING REMARKS

Experimentally determined values of the rotational and translational velocities of a sphere moving parallel to a plane wall are in good agreement with the theoretical values calculated from the exact solutions of Dean & O'Neill (1963) and O'Neill (1964). Lubrication theory and the method of reflections give results that are in agreement with the experimental data only in the limits of small and large gap widths, respectively. Our observations of the translational velocity show small deviations from the theory, similar to the findings of Ambari *et al.* (1983), but the differences can be attributed to experimental limitations at small gap widths. The observations of rotational motion at small gap widths do not show similar deviations because of the weaker dependence of the angular velocity on gap width.

REFERENCES

AMBARI, A., GAUTHIER-MANUEL, B. & GUYON, E. 1983 Effect of a plane wall on a sphere moving parallel to it. *J. Phys. Lett.* **44**, L143–146.

AMBARI, A., GAUTHIER-MANUEL, B. & GUYON, G. 1984 Wall effects on a sphere translating at constant velocity. *J. Fluid Mech.* **149**, 235–253.

CARTY, J. J., Jr. 1957 Resistance coefficients for spheres on a plane boundary. B.Sc. thesis, Massachusetts Institute of Technology.

DEAN, W. R. & O'NEILL, M. E. 1963 A slow motion of viscous liquid caused by the rotation of a solid sphere. *Mathematika* **10**, 13–24.

FAXEN, H. 1921 Einwirkung der Gerfässwände auf den Widerstand gegen die Bewegung einer kleinen Kugel in einer zähen Flussigkeit. (Diss.) Upsala, 55–128.

GOLDMAN, A. J., COX, R. G. & BRENNER, H. 1967 Slow motion of a sphere parallel to a plane wall. I. Motion through a quiescent fluid. *Chem. Engng. Sci.* **22**, 637–651.

HAPPEL, J. & BRENNER, H. 1965 *Low Reynolds Number Hydrodynamics*, pp. 286–357. Prentice-Hall, Englewood Cliffs, New Jersey.

HIRSCHFELD, B. R., BRENNER, H. & FALADE, A. 1984 First- and second-order wall effects upon the slow viscous asymmetric motion of an arbitrary-shaped, positioned and -oriented particle within a circular cylinder. *Physicochem. Hydrodynam.* **5**, 99–133.

MAŁYSA, K., DĄBROŚ, T. & VAN DE VEN, T. G. M. 1985 The sedimentation of one sphere passed a second attached to a wall. *J. Fluid Mech.*, In press.

O'NEILL, M. E. 1964 A slow motion of viscous liquid caused by a slowly moving solid sphere. *Mathematika* **11**, 67–74.